

The Acyl-Proteome of *Syntrophus aciditrophicus* Reveals Metabolic Relationships in Benzoate Degradation

Authors

John M. Muroski, Janine Y. Fu, Hong Hanh Nguyen, Neil Q. Wofford, Housna Mouttaki, Kimberly L. James, Michael J. McInerney, Robert P. Gunsalus, Joseph A. Loo, and Rachel R. Ogorzalek Loo

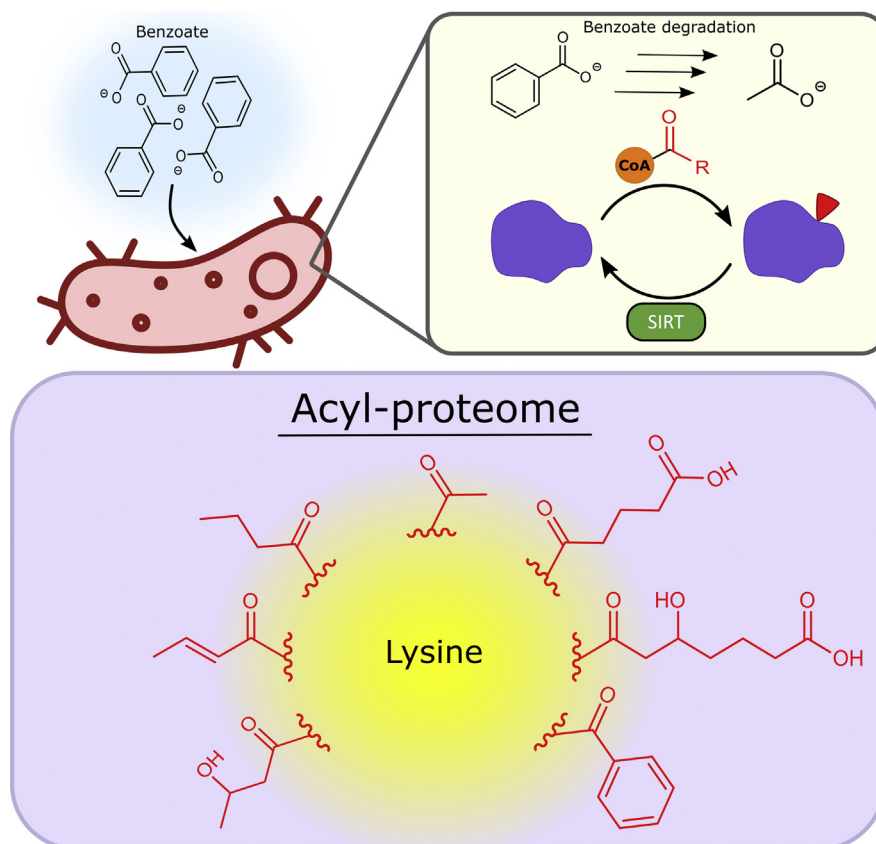
Correspondence

rloo@mednet.ucla.edu

In Brief

Syntrophus aciditrophicus is a syntrophic bacterium degrading fatty and aromatic acids into acetate, CO₂, formate, and H₂, consumed by methanogenic archaea. The syntroph's acyl-lysine modifications were analyzed with a workflow *avoiding antibody enrichment*, enabling unbiased global acylation profiling. Seven acyl modification types were identified, six corresponding to reactive acyl-CoA species intermediates in benzoate degradation. Benzoate-degrading enzymes were also prominent among the 60 acylated proteins. The abundant acylations and active deacylases suggest that post-translational modifications directly regulate syntrophic benzoate degradation.

Graphical Abstract



Highlights

- Abundant lysine modifications in microbes enable unbiased global acylation profiling.
- Seven types of acyl modifications are found; six from benzoate degradation intermediates.
- Benzoate-degrading enzymes are prominent among the 60 acylated proteins.
- Abundant acylation/active deacylases suggest PTMs modulate syntrophic metabolism.

The Acyl-Proteome of *Syntrophus aciditrophicus* Reveals Metabolic Relationships in Benzoate Degradation

John M. Muroski¹, Janine Y. Fu¹, Hong Hanh Nguyen², Neil Q. Wofford³, Housna Mouttaki³, Kimberly L. James³, Michael J. McInerney³, Robert P. Gunsalus^{4,5,6}, Joseph A. Loo^{1,5,6,7}, and Rachel R. Ogorzalek Loo^{1,5,6,*}

Syntrophus aciditrophicus is a model syntrophic bacterium that degrades fatty and aromatic acids into acetate, CO₂, formate, and H₂ that are utilized by methanogens and other hydrogen-consuming microbes. *S. aciditrophicus* benzoate degradation proceeds by a multistep pathway with many intermediate reactive acyl-coenzyme A species (RACS) that can potentially N^ε-acylate lysine residues. Herein, we describe the identification and characterization of acyl-lysine modifications that correspond to RACS in the benzoate degradation pathway. The amounts of modified peptides are sufficient to analyze the post-translational modifications *without antibody enrichment*, enabling a range of acylations located, presumably, on the most extensively acylated proteins throughout the proteome to be studied. Seven types of acyl modifications were identified, six of which correspond directly to RACS that are intermediates in the benzoate degradation pathway including 3-hydroxypimeloylation, a modification first identified in this system. Indeed, benzoate-degrading enzymes are heavily represented among the acylated proteins. A total of 125 sites were identified in 60 proteins. Functional deacylase enzymes are present in the proteome, indicating a potential regulatory system/mechanism by which *S. aciditrophicus* modulates acylation. Uniquely, N^ε-acyl-lysine RACS are highly abundant in these syntrophic bacteria, raising the compelling possibility that post-translational modifications modulate benzoate degradation in this and potentially other, syntrophic bacteria. Our results outline candidates for further study of how acylations impact syntrophic consortia.

Syntrophic bacteria serve critical roles in bioremediation and carbon cycling from anaerobic environments (1–6). They

degrade a broad range of aliphatic and aromatic acids to hydrogen, formate, CO₂, and acetate by cooperation with hydrogen- and/or formate-consuming microbes such as archaea which generate methane (2, 3). Here, the presence of methanogens and/or other hydrogen- and/or formate-consuming partners is required to maintain low hydrogen and formate concentrations, such that syntrophic substrate degradation can occur spontaneously (4). This obligate partnership between members of the microbial community exists because anaerobic degradation is thermodynamically unfavorable when hydrogen or formate levels are high (3, 5). Direct electron transfer between syntrophic microorganisms and their partner microorganisms is also possible (7). Importantly, degrading syntrophic substrates requires multiple enzymatically catalyzed reactions to be performed on many acyl-coenzyme A (CoA) intermediates. Even when hydrogen and formate levels are low, the essential acyl-CoA oxidations of syntrophic metabolism are weakly exergonic with free-energy changes close to thermodynamic equilibrium (4). The energetic challenges of living at the edge of thermodynamic feasibility make syntrophic microbes interesting models for exploring energy conservation and metabolic regulation (6).

Syntrophus aciditrophicus is an anaerobic, gram-negative bacterium that degrades fatty, aromatic, and alicyclic (cyclohexane-1-carboxylate) acids to acetate, CO₂, formate, and hydrogen when grown in coculture with hydrogen- and/or formate-consuming partner microorganisms. *S. aciditrophicus* can grow in pure culture with crotonate or benzoate (8–10) and can use benzoate as an electron acceptor to form cyclohexane-1-carboxylate (11). Previous work elucidated the

From the ¹Department of Chemistry and Biochemistry, University of California, Los Angeles, California, USA; ²TRANSMED Co Ltd, Ho Chi Minh City, Vietnam; ³Department of Microbiology and Plant Biology, University of Oklahoma, Norman, Oklahoma, USA; ⁴Department of Microbiology, Immunology and Molecular Genetics, University of California, Los Angeles, Los Angeles, California, USA; ⁵UCLA-DOE Institute, ⁶UCLA Molecular Biology Institute, and ⁷Department of Biological Chemistry, David Geffen School of Medicine, University of California, Los Angeles, California, USA

*For correspondence: Rachel R. Ogorzalek Loo, rloo@mednet.ucla.edu.

Present address for Kimberly James: Department of Microbiology and Cell Science, University of Florida, Florida 32611, USA.

Present address for Housna Mouttaki: Novartis, Sandoz GmbH, Biochemiestrasse 10, Kundl 6250, Austria.

pathways for crotonate, benzoate, and cyclohexane-1-carboxylate metabolism (12–14) and found that *S. aciditrophicus* uses many of the same enzymes to degrade and to synthesize benzoate and cyclohexane carboxylate (10, 12).

Due to challenges in isolating, manipulating, and cultivating syntrophic microorganisms, questions still remain regarding the regulatory mechanisms involved in the important anaerobic degradations. Oxidizing benzoate and other substrates generates reduced cofactors (nicotinamide adenine dinucleotide reduced and flavin adenine dinucleotide reduced) that, if unregulated, could cause stress and cellular dysfunction (15). Intermediates of substrate metabolism can also stress cells. Various acid substrates in *S. aciditrophicus* are activated through their respective CoA derivative, which serves as a scaffold through subsequent conversions, until acetate, CO₂, hydrogen, and formate are released (6, 16). The intermediates of these pathways are a series of reactive acyl-CoA species (RACS), with potential to modify the nucleophilic side chain of lysine (17). Given the multiple stressors that *S. aciditrophicus* cells experience in carbon metabolism and that its enzymes catalyze in either direction, depending on the substrate and environmental conditions (10, 12), it is suspected that previously undescribed pathway regulation is involved. The reversibility of syntrophic metabolism and its correspondingly low energy yields makes us consider that post-translational modifications (PTMs), specifically acylations associated with RACS intermediates, may play a role modulating degradations and syntheses in the cell.

Identifying and characterizing PTMs is most often done using mass spectrometry. At the systems level, proteomics can capture PTMs across all proteins, but a system presenting a wide range of acylations brings analytical complications, including potential sequence misidentifications due to isomeric and/or isobaric combinations (18, 19). Ambiguities must be addressed to confidently ascribe sequences, modifications, and modified residues in data. Increases in theoretical search space and scoring thresholds needed to satisfy false-discovery rate cutoffs for database searching are also considerations for proteomes possessing a broad variety of acylations (20).

Here, we take a systems-level approach to identify post-translational acylations associated with syntrophic benzoate metabolism by *S. aciditrophicus*. Without using PTM-specific enrichment procedures, we identify a wide range of acylations by targeting acyl-CoAs that are known to be involved in fatty and aromatic acid degradation in this and other microbes (16, 21). Using marker ions diagnostic of lysine acylation increases confidence in the PTMs identified (22). Acylations previously undocumented across the bacterial domain are identified. An understanding of how the modifications are regulated is currently lacking, although bacterial sirtuins are known to deacylate promiscuously (23, 24). To this end, we identified one sirtuin homolog (from the two present in the genome) that displays deacylase activity.

EXPERIMENTAL PROCEDURES

Media, Cultivation, and Cell Harvest

Pure cultures of *S. aciditrophicus* strain SB (DSM 26646) were grown in 500-ml Schott bottles with 250 ml of a basal medium (25) with 20 mM crotonate or 10 mM crotonate plus 2 mM benzoate. *S. aciditrophicus* was grown in coculture with *Methanospirillum hungatei* JF1 (ATCC 27890) in 2-L Schott bottles with 1 L of Tanner's mineral medium with 14 mM benzoate. Tanner's mineral medium was used for large culture volumes to avoid chemical precipitants that form in large volumes of the basal medium. Tanner's mineral medium (26) contained (per liter) 10 ml of Tanner's minerals, 5 ml of Tanner's metals, 10 ml of Tanner's vitamins, 1 ml of 0.1% resazurin, 3.75 g of NaHCO₃, and 20 ml of cysteine sulfide (2.5%) solution (27). Both media were adjusted with NaOH and HCl to pH 7.1 to 7.3. The anaerobic procedures of Balch and Wolfe (28) were used to prepare media and solutions and to inoculate and sample cultures. The headspace was pressurized with N₂/CO₂ (80%:20% v/v) to 70 kPa, and cultures were incubated at 37 °C without shaking.

Cultures were grown to mid-log phase and harvested by centrifugation (800g for 20 min at 4 °C) under strict anaerobic conditions. The cell pellet was washed twice by resuspending in 50 mM anoxic potassium phosphate buffer (pH 7.5) and centrifuging as described previously. The final cell pellet was resuspended in anoxic potassium phosphate buffer, transferred to cryovials, and stored in –80 °C (29). Culture manipulations were performed in an anaerobic Coy chamber, and all centrifuge steps were done with sealed, anoxic, centrifuge tubes (28).

Two-Dimensional Polyacrylamide Gel Electrophoresis of *S. aciditrophicus*

Two-dimensional polyacrylamide gel electrophoresis (2D-PAGE) was performed, and protein-containing spots identified as described in the Supplemental Materials section of the study by James *et al.* (12).

Preparing Tryptic Peptides for Non-Gel-Based Proteomics

S. aciditrophicus SB coculture with *M. hungatei* JF1 on benzoate substrate was described previously (12, 29). Frozen cell pellets were resuspended in lysis buffer containing 4.0% (v/v) ammonium lauryl sulfate, 0.1% sodium deoxycholate (w/v), 5 mM tris(2-carboxyethyl) phosphine, and 100 mM ammonium bicarbonate (ABC). Proteins were digested via the enhanced filter-aided sample preparation method, similar to that described by Erde *et al.* (30, 31). Briefly, lysate was buffer-exchanged into 8 M urea, 0.1% (w/v) sodium deoxycholate, and 0.1% (w/v) *n*-octyl glucoside using a 10-kDa Microcon ultrafiltration unit (Millipore). Proteins were alkylated with 17 mM iodoacetamide for an hour at room temperature, after which they were exchanged into 0.1% (w/v) sodium deoxycholate/0.1% (w/v) *n*-octyl glucoside in 100 mM ABC. Trypsin (1:100 w/w) was added, and the solution was incubated overnight at 37 °C. Ethyl acetate extraction was used to remove detergents, as previously described (30, 31).

The resulting peptides were separated off-line via hydrophilic interaction liquid chromatography. Fifty micrograms of peptides (quantified with Pierce Quantitative Fluorometric Peptide Assay) were deposited onto a BioPureSPN MACRO PolyHYDROXYETHYL A column (The Nest Group) in 90% acetonitrile and 150 mM ammonium formate, pH 3. Peptides were eluted in six fractions using ammonium formate buffers sequentially decreasing in organic content: 80% acetonitrile, 78% acetonitrile, 74% acetonitrile, 71% acetonitrile, 40% acetonitrile, and 35.5% acetonitrile. Fractions one and six were combined. No antibody affinity fractionations were performed to enrich acylated peptides.

Liquid Chromatography and Tandem Mass Spectrometry

Peptides were mass-measured and fragmented using high-performance liquid chromatography tandem mass spectrometry. Using an EASY nLC1000 liquid chromatography system (Thermo Scientific), peptides (200 ng) were loaded onto an Acclaim Pep-Map100 C18 trap column (Thermo Scientific, Product #16-494-6, 75 $\mu\text{m} \times 2 \text{ cm}$, 100 \AA) and separated on an Acclaim PepMap RSLC C18 analytical column (Thermo Scientific, Product #03-251-873, 75 $\mu\text{m} \times 25 \text{ cm}$, 100 \AA). Buffer A (0.1% formic acid) and buffer B (0.1% formic acid in acetonitrile) were mixed and delivered at 300 nl min^{-1} in a gradient of 3 to 20% B for 62 min, 20 to 30% B for 31 min, 30 to 50% B for 5 min, and 50 to 80% B for 2 min.

A Q Exactive (Thermo Fisher Scientific) quadrupole-orbitrap mass spectrometer was operated using data-dependent acquisition mode. MS scans (m/z 300–1800) were acquired at 70,000 resolution, with an automatic gain control target set to 1E6 and a maximum fill time of 100 ms. The ten most abundant precursor ions were dissociated sequentially using higher energy collisional dissociation at a normalized collisional energy of 27 (unless otherwise indicated), and MS/MS spectra were acquired at 17,500 resolution with an automatic gain control target of 1E5 at a maximum fill time of 80 ms. The mass spectrometry data from 2D gels were deposited to the ProteomeXchange Consortium via the PRIDE partner repository with dataset identifier PXD025631. Shotgun datasets submitted through MassIVE are identified as PXD025603.

Database Searching

Q Exactive *.RAW files were analyzed using ProteomeDiscoverer (version 1.4) employing Matrix Science's Mascot search algorithm (32). A database concatenating UniProt *S. aciditrophicus* and *M. hungatei* protein sequences (as of July 8, 2019) to the sequences of common contaminants was used for searches. The total number of entries in this database was 6479. Parameters used for the search were enzyme name, trypsin; maximum missed cleavage sites, two; precursor mass tolerance, 10 ppm; fragment mass tolerance, 0.02 Da; and variable methionine oxidation and cysteine carbamidomethylation. Searches also considered variable acyl-lysine modifications, all of which are shown in Table 1. These modifications were selected from RACS identified in the aromatic acid-degrading pathways of a variety of bacteria. Spectra matched to acylated peptides with Mascot ion scores ≥ 20 were subjected to manual examination, the criteria of which prioritized the presence of immonium ions and product ions spanning the modification as well as from regions that do not contain the modification. A score of 20 is associated with an expectation value of ≥ 0.1 , chosen to broadly collect spectra of potentially modified peptides.

Bioinformatic Analyses

The Kyoto Encyclopedia of Genes and Genomes (KEGG) database was used to annotate relevant pathways associated with the acylated proteins identified. UniProt accessions were converted to KEGG identifiers and mapped to the KEGG pathway database using KEGG Mapper (33). To identify Gene Ontology (GO)/KEGG pathways frequently represented by acylated proteins, functional enrichment was performed by the StringApp (version 1.6.0) in Cytoscape (version 3.8.2), and p -values were corrected for multiple testing within each category using the Benjamini-Hochberg procedure (34).

To identify sequence motifs enriched in acylated peptides, the motif-x algorithm (35) integrated into the MoMo Modification Motifs program (version 5.3.0) on the MEME suite platform (36) was used to examine sequences of acyl-21-mers (ten amino acids upstream and downstream of the corresponding acylation site) (37) from the UniProt *S. aciditrophicus* database. The other parameters were set to default

values: p -value threshold: 0.000001, the minimum number of occurrences for residue/position pair: 10.

All acylated proteins identified were searched against the STRING database (version 11.0) to reveal potential protein-protein interactions (PPIs) (38). Only protein interactions found among the acylated proteins were selected, removing any external candidate interactions. Only interactions with at least medium confidence (>0.4) were included. The interaction network was visualized in Cytoscape (version 3.8.2).

Cloning, Expression, and Purification of Syn_00042 and Syn_01020

Two *S. aciditrophicus* sirtuin candidate genes annotated as *sir2* family proteins were identified in the genome by homology search. The genes were obtained via polymerase chain reaction (PCR) of genomic DNA, cloned into plasmid pMAPLE21, and expressed in *Escherichia coli* strain BL21 as previously described by Arbing *et al.* (39). The recombinant proteins were purified by Ni-affinity chromatography followed by size exclusion (Superdex 75) and Q-Sepharose anion exchange. Purity was greater than 95% as visualized by SDS-PAGE. The apparent protein sizes were consistent with the predicted gene/protein sizes.

Sirtuin Assay (anhydride)

Acyl-insulins were prepared from the corresponding acyl-anhydrides; for example, glutaric anhydride was used for glutaryl-lysine, using methods adapted from Baeza *et al.* (40). About 25 μmol of anhydride was added to 100 μl of a 1-mg/ml solution of human insulin (Alfa Aesar, J67626) in 100 mM ABC. After incubating at 4 $^{\circ}\text{C}$ for 20 min, the solution was readjusted to pH ~ 8 using an ammonium hydroxide solution. Anhydride addition, incubation, and pH adjustment were repeated twice more. Ostensible O-acylation was reversed by adding 50% w/v of hydroxylamine hydrochloride in H_2O (adjusted with ammonium hydroxide to pH 7–8). Following overnight, room-temperature incubation, the modified products were buffer-exchanged into 100 mM ABC using 3-kD molecular weight cut-off Amicon spin filters (Millipore).

For the matrix-assisted laser desorption/ionization (MALDI)-based activity assay, an approximately 27 μM solution of acyl-modified insulin was mixed with 0.24 μM recombinantly expressed SYN_00042 and excess oxidized nicotinamide adenine dinucleotide (NAD^+) in 100 mM ABC. The solution was incubated at 37 $^{\circ}\text{C}$ for 2 h. Sample aliquots were mixed 1:1 with saturated sinapinic acid in 50% acetonitrile/0.1% trifluoroacetic acid and spotted onto a MALDI sample stage. MALDI mass spectra were obtained with an Applied Biosystems Voyager-DE STR time-of-flight mass spectrometer.

Time-series measurements of glutaryl-insulin masses used a Synapt G2-Si quadrupole time-of-flight mass spectrometer (Waters) with electrospray ionization. The assay was performed at 37 $^{\circ}\text{C}$ for the period of time indicated and quenched with 50% acetonitrile. The glutaryl-insulin was diluted to a final concentration of 10 μM for mass analysis with 20 μM ubiquitin added as internal standard. The solution was delivered by direct infusion.

Experimental Design and Statistical Rationale

S. aciditrophicus cells were grown in pure culture on crotonate as a sole carbon source or with crotonate/benzoate to analyze via 2D-PAGE. Cells were cocultured with *M. hungatei* and grown on benzoate for mass spectrometry proteomic analysis. Three samples from each culture condition were grown, and for each biological sample, three technical replicates were analyzed. As the priority was to maximize the identification of potentially low stoichiometry PTMs, offline hydrophilic interaction liquid chromatography was used to increase the depth of the identifiable proteome. Resulting data were searched for the acyl

TABLE 1
Acylation considered

Acyl modification	Chemical formula	Monoisotopic mass shift	Average mass shift	Immonium ion	Cyclized immonium ion
Acetyl	C ₂ H ₂ O	42.01056	42.03677	143.1179	126.0913
Crotonyl	C ₄ H ₄ O	68.02621	68.07413	169.1336	152.1070
Acetoacetyl	C ₄ H ₄ O ₂	84.02113	84.07353	185.1285	168.1019
Succinyl	C ₄ H ₄ O ₃	100.016	100.0729	201.1234	184.0968
Butyryl	C ₄ H ₆ O	70.04186	70.09001	171.1492	154.1226
3-Hydroxybutyryl	C ₄ H ₆ O ₂	86.03678	86.08942	187.1441	170.1176
Glutaconyl	C ₅ H ₄ O ₃	112.016	112.0837	213.1234	196.0968
Glutaryl	C ₅ H ₆ O ₃	114.0317	114.0996	215.1391	198.1125
Benzoyl	C ₇ H ₄ O	104.0262	104.1063	205.1336	188.1070
Cyclohexa-1,5-diene-1-carboxyl	C ₇ H ₆ O	106.0419	106.1222	207.1493	190.1227
6-Oxocyclohex-1-ene-1-carboxyl	C ₇ H ₆ O ₂	122.0368	122.1216	223.1442	206.1176
Cyclohex-1-ene-1-carboxyl	C ₇ H ₈ O	108.0575	108.1381	209.1649	192.1383
6-Hydroxycyclohex-1-ene-1-carboxyl	C ₇ H ₈ O ₂	124.0524	124.1375	225.1598	208.1332
2-Oxocyclohexane-carboxyl	C ₇ H ₈ O ₂	124.0524	124.1375	225.1598	208.1332
2-Heptenediyl	C ₇ H ₈ O ₃	140.0473	140.1369	241.1547	224.1281
3-Oxopimelyl	C ₇ H ₈ O ₄	156.0423	156.1363	257.1497	240.1231
Cyclohexane-1-carboxyl	C ₇ H ₁₀ O	110.0732	110.154	211.1806	194.1540
2-Hydroxycyclohexane-carboxyl	C ₇ H ₁₀ O ₂	126.0681	126.1534	227.1755	210.1489
Pimelyl	C ₇ H ₁₀ O ₃	142.063	142.1528	243.1704	226.1438
3-Hydroxypimelyl	C ₇ H ₁₀ O ₄	158.0579	158.1522	259.1653	242.1387

modifications shown in Table 1. To identify PTMs, mass spectra matched to acylated peptides with Mascot ion scores ≥ 20 were subjected to manual examination. Modifications were considered present if the tandem mass spectra included acyl-lysine-associated immonium ions (22).

RESULTS

2D-Gel Analyses Suggest Proteins Are Modified Heterogeneously

S. aciditrophicus cell lysates from axenic cultivation on benzoate supplemented with crotonate (9) were harvested and subjected to 2D-PAGE (Fig. 1) (41, 42). Spots were excised, digested with trypsin in-gel, and identified using tandem mass spectrometry (12). Frequently, spots were composed of multiple proteins, limiting the value of densitometry for evaluating abundance. In some spots, MS identified seven or more proteins with two or more tryptic peptides (or a single tryptic peptide identified from an MS/MS spectrum matched to that in a different spot, known to contain that protein, displaying 2+ tryptic peptides) (supplemental Table S1). Abundant proteins are listed in Table 2. Within the darkest spots, some MS heterogeneity suggestive of small variations in sequence was also observed, potentially reflecting high error rates in transcription and/or translation. Little is known about this latter effect.

These analyses revealed many instances in which the same protein was identified from multiple spots at the same molecular size but different isoelectric points. This pattern, often seen with glycoproteins (43), suggests heterogeneous PTMs, but we found no evidence of *S. aciditrophicus* glycoproteins.

Spot trains might strike some as reminiscent of carbamylation, but the artifacts were easily ruled out. Trains do not accompany every spot, and MS/MS analyses found protein carbamylation to be insignificant. Some of these proteins were identified as housekeeping proteins (Table 2), while others have roles in the catabolism of benzoate and other aromatic and fatty acids. Given the high abundance of RACS in these pathways, acyl-lysine modifications were considered possible. Acylation will neutralize the positive charge on lysine, or, in the cases of acidic RACS, such as glutaryl-CoA, will switch lysine to a negatively charged site. Both types of acylation reduce protein isoelectric points, shifting migration toward the anode (the left in standard 2D gel images); hence, a distribution of many and differently charged acylations would give a pattern similar to that seen in Figure 1.

Digests for spot 20 (Fig. 1) established that the acetylated and nonacetylated peptides YGTK^{ac}PEDLALIR and YGTK-PEDLALIR of the acetyl-CoA acetyltransferase SYN01681 were both present. That both acetylated and nonacetylated lysines were present could suggest that migration-compensating acylations or modifications reside at other sites on some of the SYN01681 protein in this spot. From spot 21, peptides TAVGAFGGSLK^{ac}GVR and M^{ox}AK^{ac}LAPVFK of the acetyl-CoA acetyltransferase SYN02642 were observed bearing acetyl lysines. Nonacylated TAVGAFGGSLK and LAPVFK were also observed in the spot, but at lower signal levels. Two acetylated sites were also observed from SYN01310 in spot 22, from peptides ATEEFK^{ac}QLGK and LM^{ox}AGSIK^{ac}K of 3-hydroxyacyl-CoA dehydrogenase. A corresponding unmodified peptide, GYYTSETFKATEEFK,

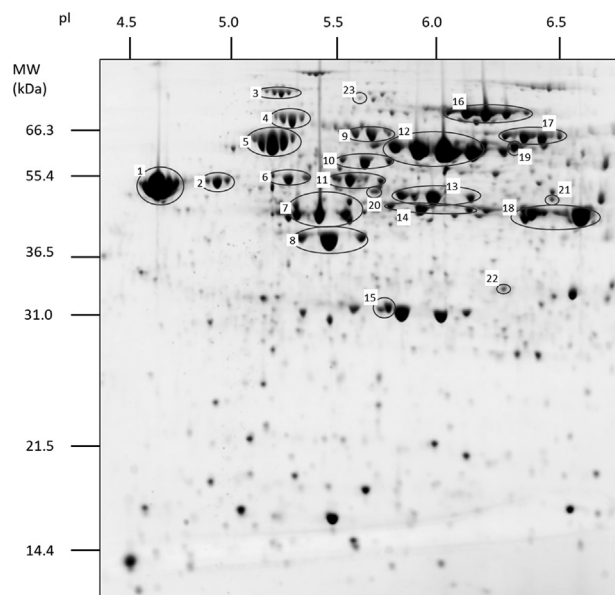


FIG. 1. Proteomic patterns of *S. aciditrophicus* as detected by 2D-PAGE. Two-dimensional gel analysis of the *S. aciditrophicus* proteome for cells grown on benzoate supplemented with crotonate. The x-axis is separated by isoelectric focusing (IEF), whereas the y-axis is separated by SDS-PAGE. Selected proteins present in the spots are listed in Table 2. 2D-PAGE, two-dimensional polyacrylamide gel electrophoresis.

was also observed in this spot, although neither unacetylated LMAGSIK nor LM^{OX}AGSIK was found. From the spot 23 proteins SYN_01788 and SYN_02636, acetylated peptides TAAALEALEK^{ac}R and YASLPGIMK^{ac}AK were detected, respectively. Unacetylated TAAALEALEK was also detected from the digested spot, but not the unacetylated SYN_02636 peptide. Most interestingly, peptide TATGK^{ac}IQR, found in spot 19, could be attributed to SYN02896 and/or SYN02898. These benzoate-CoA ligases are 77% identical and are both present in this spot, as ascertained from their unique peptides. Despite strong signals from the acylated peptide, no unacetylated peptides spanning the TATGK segment were recovered. Supplemental Spectra S1 present annotated tandem mass spectra from spots 20 to 24.

Shotgun Proteomics Identifies Many Acyl Modifications in the *S. aciditrophicus* Proteome

Three biological replicates of protein lysates from *S. aciditrophicus*/*M. hungatei* cocultures utilizing benzoate as the carbon source were analyzed in three technical replicates each by liquid chromatography tandem mass spectrometry data-dependent acquisition (supplemental Tables S2 and S3). Analyses for one biological replicate incorporated stepped collision energies to increase the diagnostic immonium ion abundances from acyl-lysines (22). Speculating that peptides acylated by reactive intermediates from benzoate degradation might be observable, we sought evidence by including

TABLE 2
Proteins identified in two-dimensional gel spots

Spot number	Locus tag	Protein function
1	SYN_03116	Hypothetical exported protein
2	SYN_00544	ATP synthase beta chain
3	SYN_02966	Phosphoenolpyruvate synthase
4	SYN_01983	Chaperone protein
5	SYN_03223	60-kDa chaperonin
6	SYN_00198	Porin
7	SYN_01709	Ketol-acid reductoisomerase
8	SYN_00480	Acyl-CoA dehydrogenase
9	SYN_01909	60-kDa chaperonin 3 (GroEL3)
10	SYN_00546	ATP synthase subunit alpha 1
11	SYN_00983	Elongation factor Tu
12	SYN_02896	Benzoate-CoA ligase (Bcl2)
13	SYN_01681	Acetyl-CoA acetyltransferase
14	SYN_02586	Cyclohexane-1-carbonyl-CoA dehydrogenase
15	SYN_01653	Enoyl-CoA hydratase
16	SYN_02635	Acetyl-CoA synthetase (Acs1)
17	SYN_03128	Cyclohexane-1-carboxylate-CoA ligase (12)
18	SYN_01654	6-Oxocyclohex-1-ene-1-carbonyl-CoA hydrolase
19 ^a	SYN_02898, SYN_02896	4-Hydroxybenzoate-CoA ligase/ benzoate-CoA ligase (Bcl2)
20 ^a	SYN_01681	Acetyl-CoA acetyltransferase
21 ^a	SYN_02642	Acetyl-CoA acetyltransferase
22 ^a	SYN_01310	3-Hydroxyacyl-CoA dehydrogenase
23 ^a	SYN_01780, SYN_02636	Polyribonucleotide nucleotidyltransferase, electron transfer flavoprotein beta-subunit

Gel spots numbered in Figure 1 were excised, and their identities determined by mass spectrometry on a QStar-XL quadrupole time-of-flight mass spectrometer.

^aDenotes proteins identified that were acetylated.

acylation mass shifts in database searches. Table 1 illustrates the acylation shifts that were considered known intermediates for *S. aciditrophicus*, for related organisms, and common acylations. A total of 125 sites were identified in 60 different proteins, and each site was modified by at least one of the acyl groups (supplemental Tables S4 and S5; supplemental Spectra S2). Acylated peptides comprise 3.2% of the unique peptides identified (supplemental Table S3). The acetylated and 3-hydroxypimelylated species predominated in both numbers of proteins and numbers of modified sites. All of the PTMs found in each biological replicate are listed in Table 3, along with information about the supporting immonium ions. Acylations corresponding to seven of the 20 searched intermediates were found (Table 3). Modifications were detected in biological replicates reproducibly (supplemental Fig. S1 and supplemental Table S4). Peptides with missed cleavages enabled elution time comparisons between modified peptides and their unmodified counterparts. Twenty-eight of these peptide pairs were identified; in 26 pairs, the acylated peptide eluted later by an average of 9.37 min (supplemental Table S6).

TABLE 3
Summary of acyl-lysine modifications identified in *S. aciditrophicus*

Modification	Proteins identified	Sites identified	Cyclized immonium ion <i>m/z</i>	Peptides with cyclized immonium ion (%)
Benzylation	1	2	188.107	100%
3-Hydroxypimelylation	16	20	224.129, 242.139	75%, 55%
Glutarylation	4	6	198.112	100%
Crotonylation	2	2	152.107	100%
3-Hydroxybutyrylation	4	6	170.118	83%
Acetylation	48	104	126.091	94%
Butyrylation	3	3	154.123	33%

For each type of modification, the number of unique proteins bearing the modification and the total number of sites observed to be modified are presented. For the modified sequences, the percentages of MS/MS spectra that contained the diagnostic ions are stated.

PTMs can be misidentified in complex proteomic datasets due to chimeric precursors, isobaric peptides, spectral complexity, and insufficient sequence-related ions (18). The large search space traversed in seeking multiple, variable modifications from shotgun datasets challenges confident assignments. To meet these challenges, we relied upon the presence of immonium ions specific for each putative acyl modification. Immonium and immonium-like ions are strong indicators of acyl-lysine (22). Proportions of putative acyl-modified spectra displaying diagnostic immonium ions are presented in Table 3. We also examined sequences upstream and downstream of each acylated residue to determine if there were sequence preferences for these modifications, and indeed, we found that nearby glycines favored lysine acetylation (supplemental Fig. S3).

Pathway Analysis of Modified Proteins

A functional annotation analysis classified proteins by KEGG pathways and GO. The GO functional classification grouped acylated proteins into three categories: biological process, molecular function, and cellular component. Most acylated proteins mapped onto KEGG pathways had roles in metabolic processes, as expected. Benzoate degradation, oxidative phosphorylation, and carbon metabolism were highly enriched (Fig. 2A). GO enrichment analyses of all acylated proteins revealed biological processes primarily related to the synthesis of metabolites, as well as energy production (Fig. 2B). Processes related to nucleotide metabolism were also highly enriched, in line with recent reports that nucleotide-binding regions increase acylation of proximate lysines (44). Altogether, the findings suggest that these acylated proteins are generally involved in carbon metabolism, degrading aromatic and fatty acids.

Acyl-lysine modifications have been shown to impact PPIs and affect the formation of enzyme complexes, altering their role in cellular physiology. To determine connections between the acylated proteins and to elucidate their functional PPI networks, we generated an interaction network based on the STRING database, visualized through Cytoscape (Fig. 2C). Within the network, there are two highly interconnected clusters, benzoate degradation and oxidative phosphorylation

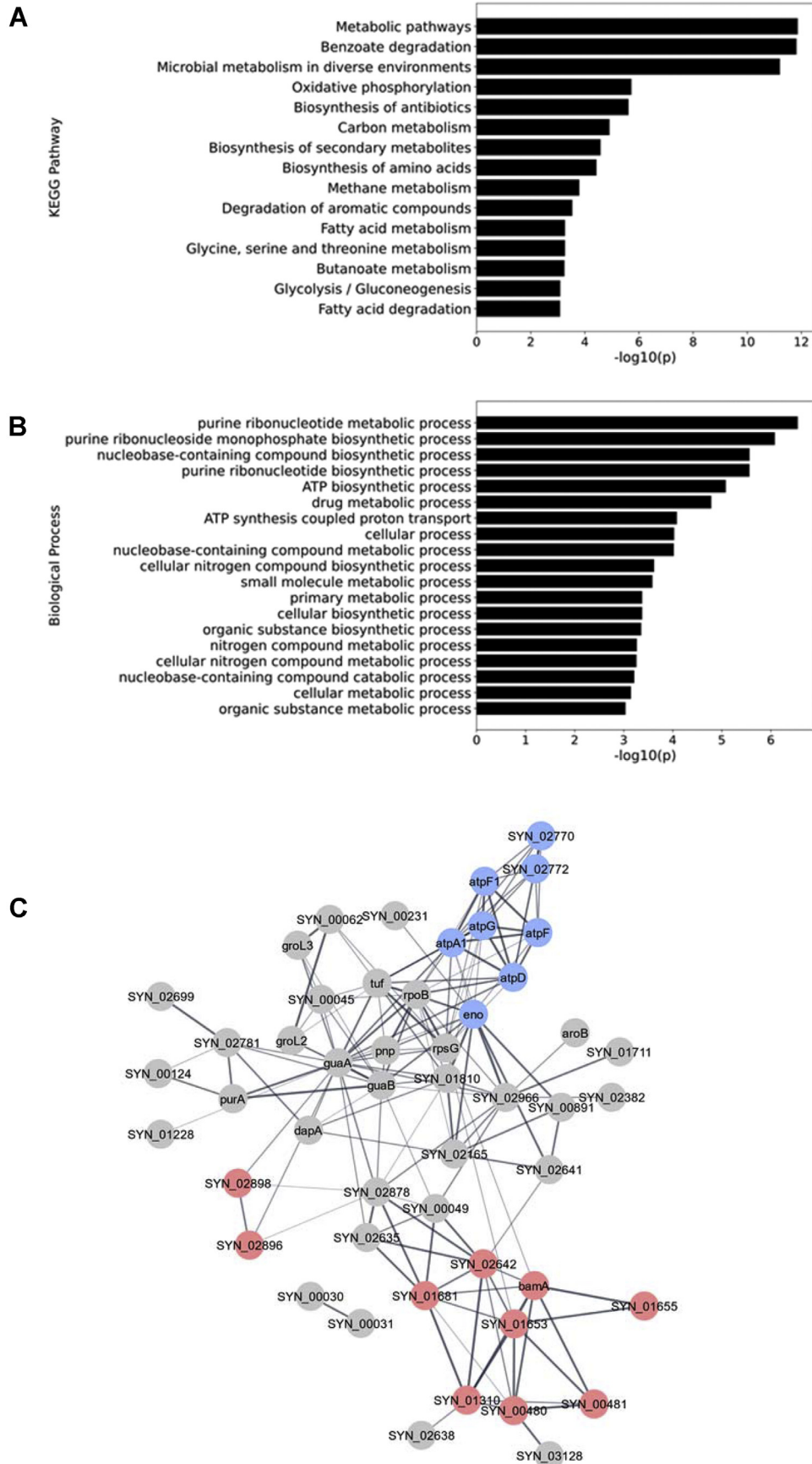
(Fig. 2C). These strong physiological interactions among all modified proteins led us to further investigate the role of protein acylation in the degradation of aromatic compounds.

Benzoate Degradation Enzymes Are Heavily Acylated

Proteins across many pathways are modified by different acyl groups at varying levels, summarized by the heat map in Figure 3A. Acetylation is found in the widest range of functional pathways, with the highest number of acetyl-lysines found in proteins related to the biosynthesis of secondary metabolites. Other acyl modifications are enriched in benzoate degradation pathway proteins, corresponding to the reactive acyl-CoA intermediates from the pathway (16). These findings imply that high local concentrations of intermediates may modify proteins spontaneously.

The largest number and widest variety of acyl modifications were found in benzoate degradation (Fig. 3B). Ten different proteins in the pathway were observed bearing several different acyl modifications. Acylated proteins included benzoate-CoA ligase, the initial step in the pathway. Several of the other acylated proteins are members of gene clusters involved in benzoic acid metabolism (*bam* genes) that are found in numerous anaerobic delta-proteobacteria (45, 46). The gene products of *bamR* (SYN_01653), *bamQ* (SYN_01655), and *bamA* (SYN_01654), which successively reduce cyclohexa-1,5-diene-1-carboxyl-CoA to 3-hydroxypimelyl-CoA, display modifications. All three gene products are acetylated, those of *bamQ* and *bamA* are glutarylated and 3-hydroxypimelylated, and that from *bamA* is also 3-hydroxybutyrylated and benzylation. Interestingly, all five modifications for the *bamA* product occur at the same site, lysine 261 (supplemental Fig. S3 and supplemental Spectra S2). Peptides containing these lysine residues were also observed unmodified.

S. aciditrophicus uses acetyl-CoA synthetase (*acs1*, SYN_02635) to make adenosine triphosphate (ATP) from acetyl-CoA. Other bacteria, in contrast, use phosphate acetyltransferase and acetate kinase, enzymes that are absent in the *S. aciditrophicus* genome. Using *acs1* to produce ATP is also remarkable because acetyl-CoA synthetases were previously thought to function only in activating acetate to



acetyl-CoA, not in the reverse direction (ATP-forming direction) (29). The rates at which ATP is produced when acetyl-CoA is the limiting substrate differ between purified and recombinantly expressed Asc1 (V_{max} of 7.5 and 1.2, respectively and K_m of 0.41 and 1.34 mM, respectively) (29), suggesting that there are factors associated with the *in vivo* protein that are not recapitulated when the enzyme is recombinantly expressed. PTMs may be one such factor. Indeed, six different sites on this protein were seen in acylated forms, all of which included acetylation, except for one site that was only butyrylated.

Proteins involved in energy conservation were also heavily acetylated. ATP synthase, Atp1, is a large complex that contains many components. Acetylation sites were identified from several subunits of Atp1, namely on the alpha (SYN_00546), beta (SYN_00544), and gamma (SYN_00545) chains (supplemental Table S5). Two homologs of ATP synthase B (the beta subunit) were also acetylated (SYN_00548 and SYN_00549).

Benzoate-CoA Ligase Reveals a Highly Modified Residue in a Conserved Region

Five of the seven acyl modifications identified in *S. aciditrophicus* proteins appeared in the sequence TATG-KIQR, present in paralogs Bcl1 (SYN_02898) and Bcl2 (SYN_02896), which differ in their activity toward different fatty and aromatic acids. The modified lysine is critical to benzoate-CoA ligase (BCL) function (47, 48), catalyzing the first step of benzoate degradation. Immonium ions present in the spectra shown in Figure 4A confirm that the unique mass shifts do, indeed, result from acylation and are not induced by mis-identifications that may result from additive side reactions that occur during sample processing; for example, formylation from exposure to high concentrations of formic acid or 12-Da mass shifts from exposure to formaldehyde (49, 50). This modification site was further investigated to determine what functional role, if any, the PTMs play. Basic Local Alignment Search Tool (BLAST) sequence alignments against closely related BCLs (47) indicated that the lysine falls in a highly conserved region (Fig. 4B). Previous *Burkholderia xenovorans* structural studies of benzoate-bound BCL (Bxe_A1419), a homolog with 46% sequence identity to Bcl1 and 44% to Bcl2, indicated that this conserved lysine is located near the benzoate carboxyl (Fig. 4C) and is hypothesized to coordinate to benzoate during enzymatic activity (47). Acylation both neutralizes the ϵ -amino side chain and adds a bulky group disrupting coordination to the carboxylate. The *Rhodospseudomonas palustris* BCL (BadA), with 43% sequence identity to Bcl1 and 42% to Bcl2, has also been found acetylated at that residue (K512). Studies *in vitro* established that

acetylation abolishes enzymatic activity (48), suggesting possible feedback inhibition of the enzyme and, in turn, the pathway.

S. aciditrophicus Sirtuins Deacylate Promiscuously

Given the ubiquity of acyl modifications in *S. aciditrophicus*, an ability to control and/or regulate acyl modifications would seem to be advantageous and critical. Sirtuin proteins have been shown to possess generalized deacylase activity, often promiscuous with respect to both sequence context and acyl modification (23, 51, 52). Bacterial systems that contain sirtuin homologs are typically denoted as *cobB* or as SIR2 family (24, 53). To determine if a deacylase capability is present, the *S. aciditrophicus* genome was searched with BLAST to determine if *E. coli cobB* homologs were present and SYN_00042 and SYN_01020 were found. A sequence alignment between these proteins displays their similarities (supplemental Fig. S4). SYN_00042 and SYN_01020 were recombinantly expressed to assay activity by mass spectrometry (Experimental Procedures).

Insulin, a dual-chain protein with one lysine and two free NH_2 -termini, was synthetically acylated using acyl anhydrides. Insulin was selected as it only has a single lysine residue and has been well characterized as a standard protein used in intact mass spectrometry work. Acylated insulin was incubated with recombinantly produced SYN_00042 and its cofactor, NAD^+ . MALDI mass spectra of glutarylated insulin showed a 114-Da decrease in mass after incubation with SYN_00042 (Fig. 5A and supplemental Table S7). The recombinant protein displayed deacylase activity against butyryl and succinyl acylations, as well (supplemental Fig. S5 and supplemental Table S7, A–G), but did not appear to act on shorter acetyl or propionyl chains. A quantitative assay of SYN_00042 gene product deacylase activity on glutaryl-insulin, performed by electrospray ionization MS, clearly shows time-dependent deglutarylase activity (Fig. 5B and supplemental Table S7, H–M). SYN_01020 was expressed in an attempt to assess its function, but did not display reproducible activity.

DISCUSSION

PTMs can modulate protein function in response to cellular or environmental changes and may occur spontaneously due to cellular conditions or simply over time (17, 54–56). Acylation is one class of modification that can be spontaneously induced in the presence of acyl phosphate or RACS or can be enzyme-mediated by a lysine acyltransferase (KAT) (57). Regardless of its origin, acylation can affect enzymatic activity profoundly. *In vitro* work has shown that modifying lysine side

FIG. 2. **Functional enrichment of acylated proteins.** A, Gene Ontology biological processes that are enriched. B, enriched KEGG pathway processes. C, a functional protein association network generated using the STRING database. Proteins involved in oxidative phosphorylation are colored in blue. Proteins involved in degrading benzoate are red. KEGG, Kyoto Encyclopedia of Genes and Genomes.

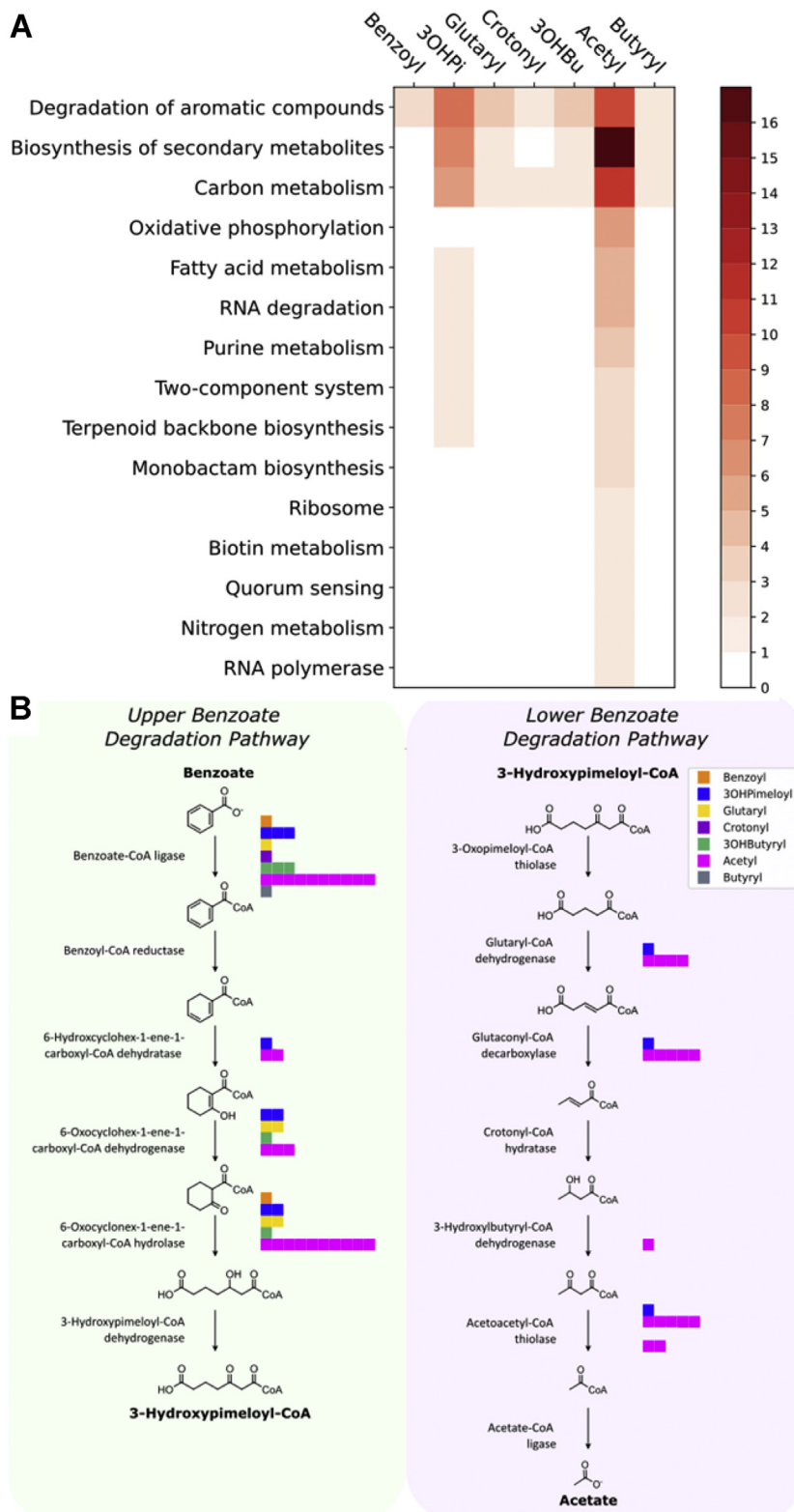


FIG. 3. Mapping sites of protein lysine acylation based on COG functional pathway analysis. *A*, a heatmap indicating the pathways (KEGG Ontology) involved for the acyl-modified protein identified. The color indicates the number of proteins in each category that have the specified acylation. *B*, modified sites identified in the “upper” and “lower” benzoate pathway. Bar plots illustrate the range of modifications found on associated enzymes. One square indicates one site of modification, and each color represents a different acylation. RACS modification types are indicated in the upper right corner boxed color code. COG, clusters of orthologous groups; KEGG, Kyoto Encyclopedia of Genes and Genomes; RACS, reactive acyl-coenzyme A species.

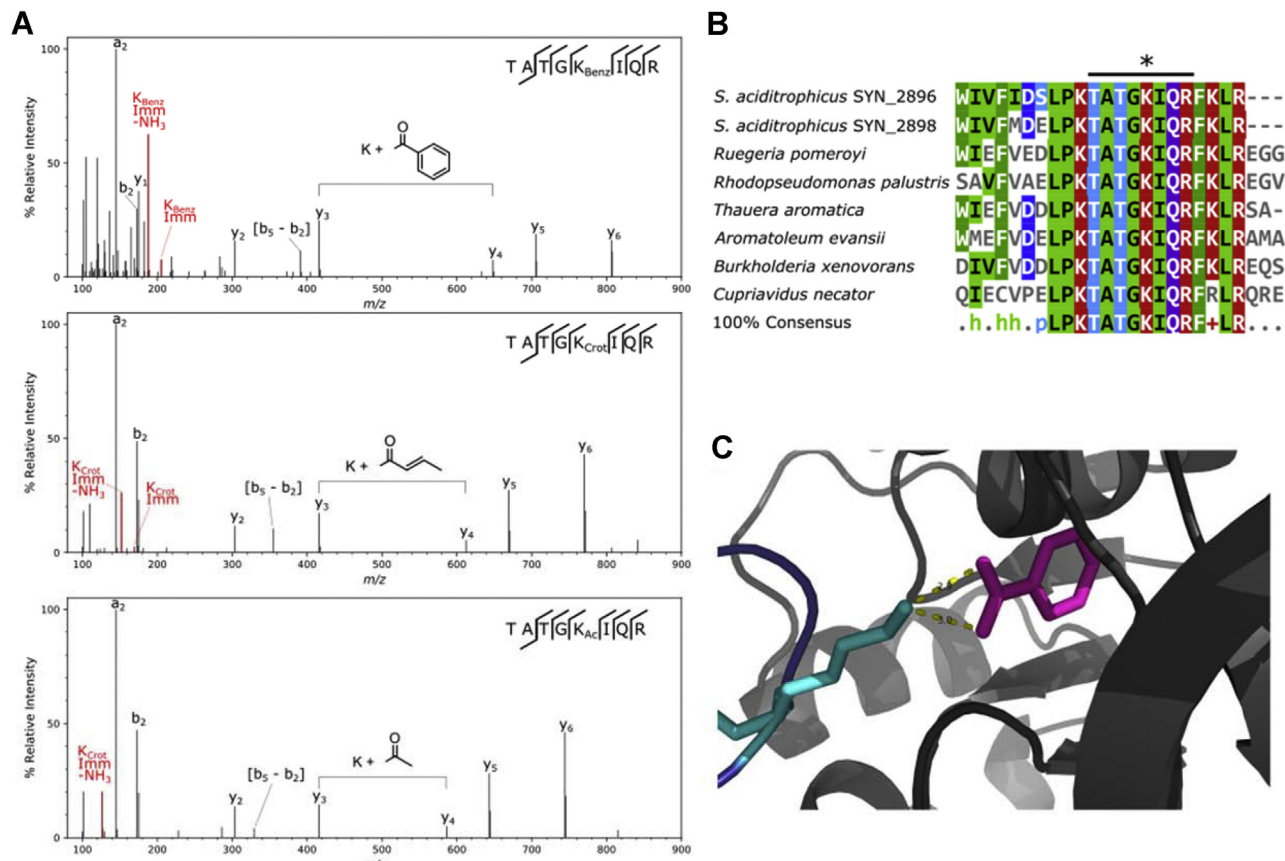


FIG. 4. Modified benzoate-CoA ligase (BCL). A, HCD spectra of acylated TATGKIQR from SYN_02896 and SYN_02898. The benzoylated spectrum (top) was collected with a stepped NCE method of 27 V/40 V. Other spectra were collected at 27 NCE. Immonium ions of modifications are denoted in red. B, sequence alignment of known BCLs across microbial systems. The line above the sequence (TATGKIQR) denotes the peptide identified in (A). The asterisk (*) denotes the corresponding modified lysine residue identified in *S. aciditrophicus*. C, crystal structure of a closely related BCL from *Burkholderia xenovorans*, determined by Bains and Boulanger (47), indicates that the acyl-lysine is proximal to a benzoate bound to the active site. BCL, benzoate-CoA ligase; HCD, higher energy collisional dissociation; NCE, normalized collision energy.

chains near catalytic regions of bacterial enzymes can directly alter function (58–60). Work in other systems has shown more subtle but equally significant acylation effects: acetylation can disrupt enzyme complexes, thereby altering activity (61–64). Acetyl-lysine has been identified as a ubiquitous modification in bacteria (65). Most acetylated proteins in our system were involved in the synthesis of secondary metabolites (Fig. 3A), which is sensible given that acetyl-CoA is an intermediate metabolite in many of those pathways. Benzoyl- (51), glutaryl- (66), hydroxybutyryl- (67, 68), crotonyl- (69, 70), and butyryl-lysine (71, 72) have shown function in some systems under certain conditions, although the studies have been less extensive than those for acetyl-lysine, and few, if any, bacterial studies have reported their occurrence. A 3-hydroxypimelylation has previously been reported in *S. aciditrophicus* by our laboratory (22). Detecting these modifications across biological replicates without pre-enrichment suggests that they are uniquely prevalent and abundant in this system. While butyryl-CoA is not expected to be an intermediate in the degradation pathway, *S. aciditrophicus* has genes for butyrate

dehydrogenase activity (3, 8) that could synthesize butyryl-CoA from excess crotonyl-CoA or reduced cofactors (8, 12).

To begin to understand how these modifications affect global cellular function requires a comprehensive and unbiased catalog of acylations. Recording a biological system's acyl modifications comprehensively presents many challenges. Low stoichiometries of acyl modifications in many model systems have required enrichment to identify and characterize acylated peptides (66, 73–81). Pan-specific antibodies are valuable for enriching specifically modified peptides but have some limitations. Antibody cross-reactivity may lessen the modification specificity of enriched peptides, a problem for Western blotting, but not mass spectrometry. Sequence-dependent binding efficiencies can bias results and challenge quantification strategies. Our syntrophic system provides a unique opportunity to investigate the array of acylations without enrichment, bypassing technical challenges in other systems. The experimental approach described herein using RACS as a predictor for lysine acylations complements antibody

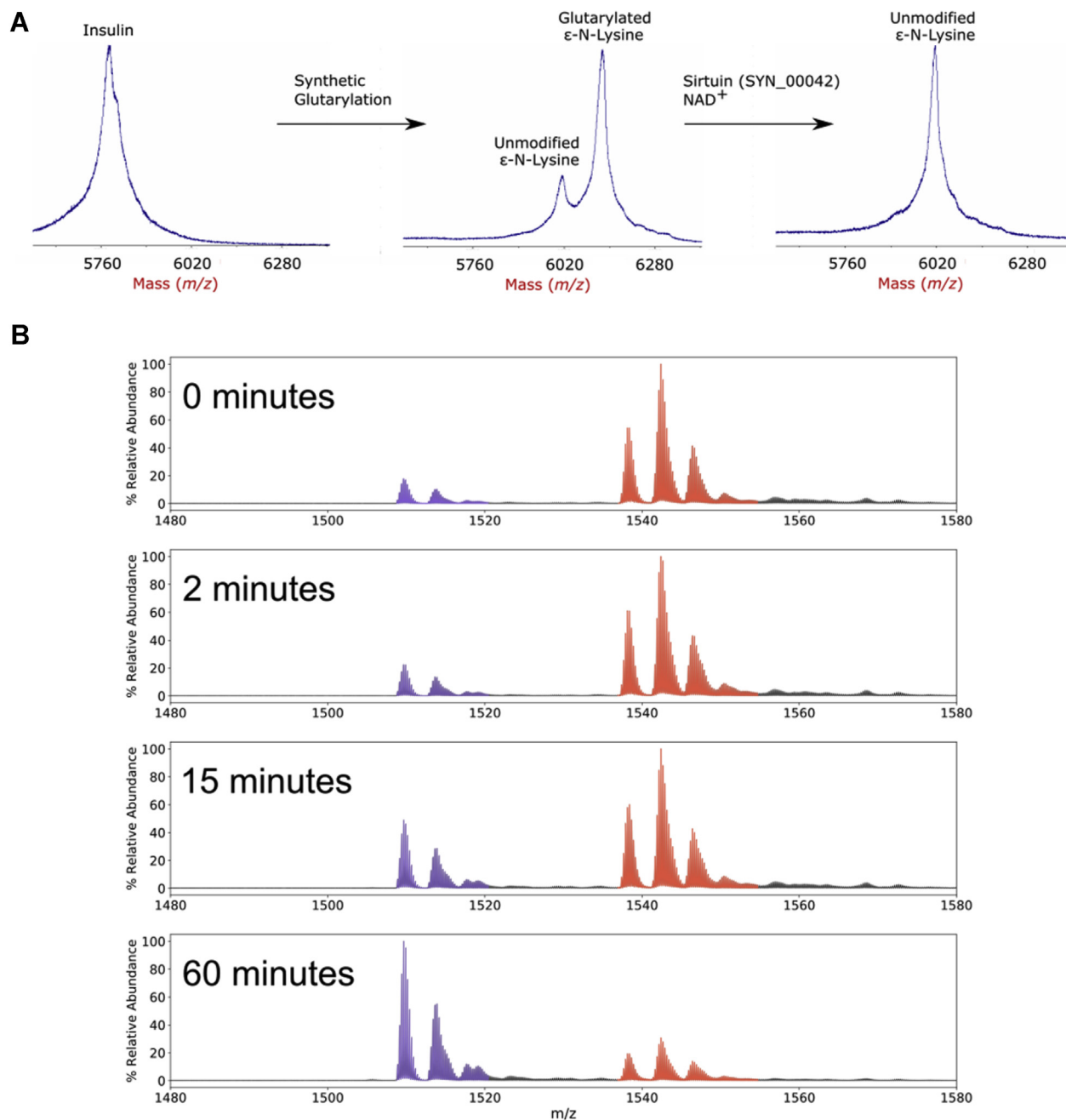


FIG. 5. *S. aciditrophicus* sirtuin SYN_00042 shows *in vitro* deacylase activity. A, MALDI-MS of insulin and modified insulin deacylated by sirtuin (Syn_00042). The peak corresponding to “Glutarylated N^ε - Lysine” reflects the mass shift from three glutaryl modifications (+342 Da), two at the N-termini and one at the single lysine. B, ESI-MS of the 4+ charge states 0, 2, 15 and 60 min after sirtuin addition. Purple peak clusters (left) correspond to insulin modified at the two N-termini; red clusters identify insulin modified at all three sites. Ammonium adducts (+17 Da) are also present. ESI, electrospray ionization; MALDI, matrix-assisted laser desorption/ionization; MS, mass spectrometry.

enrichment and utilizes diagnostic marker ions to validate putative modifications proposed from an enlarged search space.

Many of the *S. aciditrophicus* proteins decorated with acyl modifications function to degrade benzoate, a process that could result in carbon or reductive stress, if unregulated. Modulating enzymatic activity through protein acylation would

be a fitting and elegant mechanism for global metabolic regulation, given the limited energy available to these cells and the high concentrations of acyl-CoA intermediates, a feature also evidenced by the unusual ability of this species to use acetyl-CoA to form ATP (29). The benzoate degradation pathway is a likely candidate for this level of regulation as its constituents frequently interact with RACS. While we have

identified a wide range of acyl modifications in this system, the biological role that these modifications play has yet to be explored. We can, however, provide some insight into the functional effect of certain acylation sites by drawing on similar modifications in other systems. BCL acylation, specifically acetylation, has been identified as a means of negative feedback inhibition, stopping benzoate-CoA ligase activity in *R. palustris* by directly inhibiting enzymatic catalysis (48). The large number of acyl modifications we report at this site may indicate that when its respective acyl-intermediate builds, the PTM can act as a brake to slow or stop degradation, thereby acting as a negative feedback inhibitor to mitigate carbon and reductive stress. BCL also consumes ATP, creating a direct link between the energetic state of the cell and aromatic degradation. Additionally, the multiple sites of acetylation found on ATP synthase subunits further hint at a link between bioenergetics and acylation as it, too, demonstrates a relationship between the reactive metabolites and oxidative phosphorylation.

Beyond energetics, the cellular reductive state may also be regulated by the acylation of enzymes. Benzoate degradation generates nicotinamide adenine dinucleotide reduced and flavin adenine dinucleotide reduced, but excess reducing capacity stresses cells. A buildup of intermediates that subsequently modifies and slows the rates of enzymatic catalysis would safeguard against damaging reductive stress (15, 82, 83). This link is further enforced by the presence of sirtuins, whose activity is non-energy-conserving, and relies upon the oxidized cofactor NAD⁺ for activity (84), innately linking the extent of protein acylation to cellular redox state. Interestingly, the sirtuin assayed in this system appears to have a bias for longer chain acylations, particularly glutarylation, a trait that is shared with Sirt4 and Sirt5 in mammalian systems (66, 85, 86). Although *S. aciditrophicus* sirtuins were identified by homology to CobB, their activities deviate notably from those of the *E. coli* enzyme, as illustrated by their action on only longer acyl groups, not acetyl. Previous studies indicated that sirtuin specificity across species including *E. coli* CobB, mammalian Sirt5, and *Archaeoglobus fulgidus* Sir2Af2 demonstrates that while also having deacetylase activity, their selectivity toward long-chain deacylation is dependent on a YxxR motif present in the binding pocket (87, 88). However, in the *S. aciditrophicus* sirtuins, no such motif exists (supplemental Fig. S4), suggesting a different substrate selection mechanism.

The PTMs identified derive from acyl-CoA intermediates at steps which require the loss of 2 [H] (release of two reducing equivalents) (16). Hydrogen buildup is a limiting factor in the syntrophic metabolism, as is evidenced by the need for a hydrogen-scavenging partner (4). It is therefore expected that some metabolites would accumulate under high hydrogen concentrations, providing another link between the metabolic conditions of the cell and the observed acyl modifications.

Interestingly, the lower benzoate pathway degrading 3-hydroxypimelyl-CoA (Fig. 2C) is conserved across many anaerobes that degrade benzoate and other aromatic compounds (89, 90). The acyl modifications we identified on these proteins suggest that the modifications are likely present in other bacteria sharing the same or similar metabolic pathways, especially under cellular conditions that induce an accumulation of intermediates. *S. aciditrophicus* has demonstrated a wide array of acyl modifications within its proteome. Further investigation into the function of these acylations presents an opportunity to understand how these essential environmental microbes regulate their metabolism. Other syntrophs also contain critical pathways with RACS intermediates (91–93), and a wider investigation of other syntrophs may further reveal the role RACS play in bacterial metabolism.

DATA AVAILABILITY

All data were uploaded to ProteomeXchange (proteomexchange.org) either through PRIDE (2D-gel dataset; PXD025631) or through MassIVE (Shotgun dataset; PXD025603).

Supplemental data—This article contains [supplemental data](#).

Acknowledgments—We are grateful for the 2D-PAGE and mass spectrometry analyses performed by Dr Yanan Yang. We would like to thank Dr Mark Arbing and Annie Shin of the UCLA-DOE Institute Protein Expression Technology Center (supported by grant 447147-EL-21341 from the US Department of Energy) for expression and purification of *Syntrophus aciditrophicus* SYN_00042 and SYN_01020.

Author contributions—M. J. M., R. P. G., J. A. L., and R. R. O. L. conceptualization; J. M. M., H. H. N., M. J. M., R. P. G., J. A. L., and R. R. O. L. methodology; J. M. M., J. Y. F., H. H. N., N. Q. W., H. M., K. L. J., and R. R. O. L. investigation; J. M. M., J. Y. F., H. H. N., and R. R. O. L. data curation; J. M. M., J. Y. F., N. Q. W., H. M., K. L. J., M. J. M., R. P. G., and R. R. O. L. formal analysis; J. M. M., J. Y. F., M. J. M., R. P. G., J. A. L., and R. R. O. L. writing—original draft; J. M. M., J. Y. F., N. Q. W., H. M., K. L. J., M. J. M., R. P. G., J. A. L., and R. R. O. L. writing—review and editing.

Funding and additional information—Funding from the Department of Energy Office of Science (BER) contract DE-FC-02-02ER63421 (to J. A. L. and R. P. G.; UCLA/DOE Institute for Genomics and Proteomics), NIH Ruth L. Kirschstein National Research Service 18 Award (to J. Y. F.; GM007185), NSF Award 1911781 to R. P. G. and M. J. M., and NSF Graduate Research Fellowship (to J. Y. F.; DGE-1650604) are acknowledged. Also acknowledged are the National Institute of Health awards GM104610 and GM085402 to

R. O. L. and J. A. L. The content is solely the responsibility of the authors and does not necessarily represent the official views of the National Institutes of Health.

Conflict of interest—The authors declare no competing interests.

Abbreviations—The abbreviations used are: 2D-PAGE, two-dimensional polyacrylamide gel electrophoresis; ABC, ammonium bicarbonate; ATP, adenosine triphosphate; BCL, benzoate-CoA ligase; BLAST, Basic Local Alignment Search Tool; CoA, Coenzyme A; GO, Gene Ontology; KEGG, Kyoto Encyclopedia of Genes and Genomes; MALDI, matrix-assisted laser desorption/ionization; PPI, protein-protein interaction; PTM, post-translational modification; RACS, reactive acyl-coenzyme A species.

Received May 19, 2021, and in revised form, January 13, 2022
Published, MCPRO Papers in Press, February 19, 2022, <https://doi.org/10.1016/j.mcpro.2022.100215>

REFERENCES

1. Stams, A. J. M., Sousa, D. Z., Kleerebezem, R., and Plugge, C. M. (2012) Role of syntrophic microbial communities in high-rate methanogenic bioreactors. *Water Sci. Technol.* **66**, 352–362
2. McInerney, M. J., Sieber, J. R., and Gunsalus, R. P. (2009) Syntrophy in anaerobic global carbon cycles. *Curr. Opin. Biotechnol.* **20**, 623–632
3. McInerney, M. J., Rohlin, L., Mouttaki, H., Kim, U., Krupp, R. S., Rios-Hernandez, L., Sieber, J., Struchtemeyer, C. G., Bhattacharyya, A., Campbell, J. W., and Gunsalus, R. P. (2007) The genome of *Syntrophus aciditrophicus*: Life at the thermodynamic limit of microbial growth. *Proc. Natl. Acad. Sci. U. S. A.* **104**, 7600–7605
4. Schink, B. (1997) Energetics of syntrophic cooperation in methanogenic degradation. *Microbiol. Mol. Biol. Rev.* **61**, 262–280
5. Stams, A. J. M., and Plugge, C. M. (2009) Electron transfer in syntrophic communities of anaerobic bacteria and archaea. *Nat. Rev. Microbiol.* **7**, 568–577
6. Jackson, B. E., and McInerney, M. J. (2002) Anaerobic microbial metabolism can proceed close to thermodynamic limits. *Nature* **415**, 454–456
7. Walker, D. J. F., Nevin, K. P., Holmes, D. E., Rotaru, A. E., Ward, J. E., Woodard, T. L., Zhu, J., Ueki, T., Nonnenmann, S. S., McInerney, M. J., and Lovley, D. R. (2020) *Syntrophus* conductive pili demonstrate that common hydrogen-donating syntrophs can have a direct electron transfer option. *ISME J.* **14**, 837–846
8. Jackson, B. E., Bhupathiraju, V. K., Tanner, R. S., Woese, C. R., and McInerney, M. J. (1999) *Syntrophus aciditrophicus* sp. nov., a new anaerobic bacterium that degrades fatty acids and benzoate in syntrophic association with hydrogen-using microorganisms. *Arch. Microbiol.* **171**, 107–114
9. Elshahed, M. S., and McInerney, M. J. (2001) Benzoate fermentation by the anaerobic bacterium *Syntrophus aciditrophicus* in the absence of hydrogen-using microorganisms. *Appl. Environ. Microbiol.* **67**, 5520–5525
10. Mouttaki, H., Nanny, M. A., and McInerney, M. J. (2007) Cyclohexane carboxylate and benzoate formation from crotonate in *Syntrophus aciditrophicus*. *Appl. Environ. Microbiol.* **73**, 930–938
11. Mouttaki, H., Nanny, M. A., and McInerney, M. J. (2008) Use of benzoate as an electron acceptor by *Syntrophus aciditrophicus* grown in pure culture with crotonate. *Environ. Microbiol.* **10**, 3265–3274
12. James, K. L., Kung, J. W., Crable, B. R., Mouttaki, H., Sieber, J. R., Nguyen, H. H., Yang, Y., Xie, Y., Erde, J., Wofford, N. Q., Karr, E. A., Loo, J. A., Ogorzalek Loo, R. R., Gunsalus, R. P., and McInerney, M. J. (2019) *Syntrophus aciditrophicus* uses the same enzymes in a reversible manner to degrade and synthesize aromatic and alicyclic acids. *Environ. Microbiol.* **21**, 1833–1846
13. Peters, F., Shinoda, Y., McInerney, M. J., and Boll, M. (2007) Cyclohexa-1, 5-diene-1-carbonyl-coenzyme A (CoA) hydratases of *Geobacter metallireducens* and *Syntrophus aciditrophicus*: Evidence for a common benzoyl-CoA degradation pathway in facultative and strict anaerobes. *J. Bacteriol.* **189**, 1055–1060
14. Kuntze, K., Shinoda, Y., Mouttaki, H., McInerney, M. J., Vogt, C., Richnow, H. H., and Boll, M. (2008) 6-Oxocyclohex-1-ene-1-carbonyl-coenzyme A hydrolases from obligately anaerobic bacteria: Characterization and identification of its gene as a functional marker for aromatic compounds degrading anaerobes. *Environ. Microbiol.* **10**, 1547–1556
15. Mavi, P. S., Singh, S., and Kumar, A. (2020) Reductive stress: New insights in physiology and drug tolerance of *Mycobacterium*. *Antioxid. Redox Signal.* **32**, 1348–1366
16. Elshahed, M. S., Bhupathiraju, V. K., Wofford, N. Q., Nanny, M. A., and McInerney, M. J. (2001) Metabolism of benzoate, cyclohex-1-ene carboxylate, and cyclohexane carboxylate by *Syntrophus aciditrophicus* strain SB in syntrophic association with H₂-using microorganisms. *Appl. Environ. Microbiol.* **67**, 1728–1738
17. Trub, A. G., and Hirsche, M. D. (2018) Reactive acyl-CoA species modify proteins and induce carbon stress. *Trends Biochem. Sci.* **43**, 369–379
18. Kim, M. S., Zhong, J., and Pandey, A. (2016) Common errors in mass spectrometry-based analysis of post-translational modifications. *Proteomics* **16**, 700–714
19. Lee, S., Tan, M., Dai, L., Kwon, O. K., Yang, J. S., Zhao, Y., and Chen, Y. (2013) MS/MS of synthetic peptide is not sufficient to confirm new types of protein modifications. *J. Proteome Res.* **12**, 1007–1013
20. Fu, Y. (2012) Bayesian false discovery rates for post-translational modification proteomics. *Stat. Interf.* **5**, 47–59
21. Harwood, C. S., Burchhardt, G., Herrmann, H., and Fuchs, G. (1998) Anaerobic metabolism of aromatic compounds via the benzoyl-CoA pathway. *FEMS Microbiol. Rev.* **22**, 439–458
22. Muroski, J. M., Fu, J. Y., Nguyen, H. H., Ogorzalek Loo, R. R., and Loo, J. A. (2021) Leveraging immonium ions for targeting acyl-lysine modifications in proteomic datasets. *Proteomics* **21**, 2000111
23. Bheda, P., Jing, H., Wolberger, C., and Lin, H. (2016) The substrate specificity of sirtuins. *Annu. Rev. Biochem.* **85**, 405–429
24. Zhao, K., Chai, X., and Marmorstein, R. (2004) Structure and substrate binding properties of cobB, a Sir2 homolog protein deacetylase from *Escherichia coli*. *J. Mol. Biol.* **337**, 731–741
25. Sieber, J. R., Le, H. M., and McInerney, M. J. (2014) The importance of hydrogen and formate transfer for targeting fatty, aromatic and alicyclic metabolism. *Environ. Microbiol.* **16**, 177–188
26. Tanner, R. S. (2007) Cultivation of bacteria and fungi. In: Hurst, C., Crawford, R., Garland, J., Lipson, D., Mills, A., Stetzenbach, L., eds. *Manual of Environmental Microbiology*, 3rd Ed, American Society of Microbiology, Washington, DC: 69–78
27. McInerney, M. J., Bryant, M. P., and Pfennig, N. (1979) Anaerobic bacterium that degrades fatty acids in syntrophic association with methanogens. *Arch. Microbiol.* **122**, 129–135
28. Balch, W. E., and Wolfe, R. S. (1976) New approach to the cultivation of methanogenic bacteria: 2 Mercaptoethanesulfonic acid (HS CoM) dependent growth of methanobacterium ruminantium in a pressurized atmosphere. *Appl. Environ. Microbiol.* **32**, 781–791
29. James, K. L., Ríos-Hernández, L. A., Wofford, N. Q., Mouttaki, H., Sieber, J. R., Sheik, C. S., Nguyen, H. H., Yang, Y., Xie, Y., Erde, J., Rohlin, L., Karr, E. A., Loo, J. A., Loo, R. R. O., Hurst, G. B., et al. (2016) Pyrophosphate-dependent ATP formation from acetyl coenzyme a in *Syntrophus aciditrophicus*, a new twist on ATP formation. *mBio* **7**, e01208-16
30. Erde, J., Loo, R. R. O., and Loo, J. A. (2014) Enhanced FASP (eFASP) to increase proteome coverage and sample recovery for quantitative proteomic experiments. *J. Proteome Res.* **13**, 1885–1895
31. Erde, J., Loo, R. R. O., and Loo, J. A. (2017) Improving proteome coverage and sample recovery with enhanced FASP (eFASP) for quantitative proteomic experiments. *Methods Mol. Biol.* **1550**, 11–18
32. Perkins, D. N., Pappin, D. J. C., Creasy, D. M., and Cottrell, J. S. (1999) Probability-based protein identification by searching sequence databases using mass spectrometry data. *Electrophoresis* **20**, 3551–3567
33. Kanehisa, M., and Sato, Y. (2020) KEGG Mapper for inferring cellular functions from protein sequences. *Protein Sci.* **29**, 28–35
34. Doncheva, N. T., Morris, J. H., Gorodkin, J., and Jensen, L. J. (2019) Cytoscape StringApp: Network analysis and visualization of proteomics data. *J. Proteome Res.* **18**, 623–632

35. Schwartz, D., and Gygi, S. P. (2005) An iterative statistical approach to the identification of protein phosphorylation motifs from large-scale data sets. *Nat. Biotechnol.* **23**, 1391–1398
36. Bailey, T. L., Boden, M., Buske, F. A., Frith, M., Grant, C. E., Clementi, L., Ren, J., Li, W. W., and Noble, W. S. (2009) MEME Suite: Tools for motif discovery and searching. *Nucleic Acids Res.* **37**, W202–W208
37. Cheng, A., Grant, C. E., Noble, W. S., and Bailey, T. L. (2019) MoMo: Discovery of statistically significant post-translational modification motifs. *Bioinformatics* **35**, 2774–2782
38. Szklarczyk, D., Gable, A. L., Lyon, D., Junge, A., Wyder, S., Huerta-Cepas, J., Simonovic, M., Doncheva, N. T., Morris, J. H., Bork, P., Jensen, L. J., and Von Mering, C. (2019) STRING v11: Protein-protein association networks with increased coverage, supporting functional discovery in genome-wide experimental datasets. *Nucleic Acids Res.* **47**, D607–D613
39. Arbing, M. A., Chan, S., Harris, L., Kuo, E., Zhou, T. T., Ahn, C. J., Nguyen, L., He, Q., Lu, J., Menchavez, P. T., Shin, A., Holton, T., Sawaya, M. R., Cascio, D., and Eisenberg, D. (2013) Heterologous expression of mycobacterial Esx complexes in *Escherichia coli* for structural studies is facilitated by the use of maltose binding protein fusions. *PLoS One* **8**, e81753
40. Baeza, J., Smallegan, M. J., and Denu, J. M. (2015) Site-specific reactivity of nonenzymatic lysine acetylation. *ACS Chem. Biol.* **10**, 122–128
41. O'Farrell, P. H. (1975) High resolution two dimensional electrophoresis of proteins. *J. Biol. Chem.* **250**, 4007–4021
42. Ogorzalek Loo, R. R., Cavalcoli, J. D., VanBogelen, R. A., Mitchell, C., Loo, J. A., Moldover, B., and Andrews, P. C. (2001) Virtual 2-D gel electrophoresis: Visualization and analysis of the *E. coli* proteome by mass spectrometry. *Anal. Chem.* **73**, 4063–4070
43. Kleinert, P., Kuster, T., Arnold, D., Jaeken, J., Heizmann, C. W., and Troxler, H. (2007) Effect of glycosylation on the protein pattern in 2-D-gel electrophoresis. *Proteomics* **7**, 15–22
44. James, A. M., Smith, A. C., Ding, S., Houghton, J. W., Robinson, A. J., Antrobus, R., Fearnley, I. M., and Murphy, M. P. (2020) Nucleotide-binding sites can enhance N-acylation of nearby protein lysine residues. *Sci. Rep.* **10**, 20254
45. Wischgoll, S., Heintz, D., Peters, F., Erxleben, A., Samighausen, E., Reski, R., Van Dorsselaer, A., and Boll, M. (2005) Gene clusters involved in anaerobic benzoate degradation of *Geobacter metallireducens*. *Mol. Microbiol.* **58**, 1238–1252
46. Carmona, M., Zamarro, M. T., Blázquez, B., Durante-Rodríguez, G., Juárez, J. F., Valderrama, J. A., Barragán, M. J. L., García, J. L., and Díaz, E. (2009) Anaerobic catabolism of aromatic compounds: A genetic and genomic view. *Microbiol. Mol. Biol. Rev.* **73**, 71–133
47. Bains, J., and Boulanger, M. J. (2007) Biochemical and structural characterization of the paralogous benzoate CoA ligases from *Burkholderia xenovorans* LB400: Defining the entry point into the novel benzoate oxidation (box) pathway. *J. Mol. Biol.* **373**, 965–977
48. Crosby, H. A., Heiniger, E. K., Harwood, C. S., and Escalante-Semerena, J. C. (2010) Reversible Nε-lysine acetylation regulates the activity of acyl-CoA synthetases involved in anaerobic benzoate catabolism in *Rhodospirillum rubrum*. *Mol. Microbiol.* **76**, 874–888
49. Du, Y., Wang, F., May, K., Xu, W., and Liu, H. (2012) Determination of deamidation artifacts introduced by sample preparation using ¹⁸O-labeling and tandem mass spectrometry analysis. *Anal. Chem.* **84**, 6355–6360
50. Tang, L., Wu, Z., Wang, J., and Zhang, X. (2020) Formaldehyde derivatization, an unexpected side reaction during filter-aided sample preparation. *Anal. Chem.* **92**, 12120–12125
51. Huang, H., Zhang, D., Wang, Y., Perez-Neut, M., Han, Z., Zheng, Y. G., Hao, Q., and Zhao, Y. (2018) Lysine benzoylation is a histone mark regulated by SIRT2. *Nat. Commun.* **9**, 1–11
52. Mathias, R. A., Greco, T. M., Oberstein, A., Budayeva, H. G., Chakrabarti, R., Rowland, E. A., Kang, Y., Shenk, T., and Cristea, I. M. (2014) Sirtuin 4 is a lipamidase regulating pyruvate dehydrogenase complex activity. *Cell* **159**, 1615–1625
53. Tucker, A. C., and Escalante-Semerena, J. C. (2010) Biologically active isoforms of CobB sirtuin deacetylase in *Salmonella enterica* and *Erwinia amylovora*. *J. Bacteriol.* **192**, 6200–6208
54. Lindner, H., and Helliger, W. (2001) Age-dependent deamidation of asparagine residues in proteins. *Exp. Gerontol.* **36**, 1551–1563
55. Aswad, D. W., Paranandi, M. V., and Schurter, B. T. (2000) Isoaspartate in peptides and proteins: Formation, significance, and analysis. *J. Pharm. Biomed. Anal.* **21**, 1129–1136
56. Dalle-Donne, I., Aldini, G., Carini, M., Colombo, R., Rossi, R., and Milzani, A. (2006) Protein carbonylation, cellular dysfunction, and disease progression. *J. Cell. Mol. Med.* **10**, 389–406
57. Christensen, D. G., Baumgartner, J. T., Xie, X., Jew, K. M., Basisty, N., Schilling, B., Kuhn, M. L., and Wolfe, A. J. (2019) Mechanisms, detection, and relevance of protein acetylation in prokaryotes. *mBio* **10**, e02708-18
58. Christensen, D. G., Xie, X., Basisty, N., Byrnes, J., McSweeney, S., Schilling, B., and Wolfe, A. J. (2019) Post-translational protein acetylation: An elegant mechanism for bacteria to dynamically regulate metabolic functions. *Front. Microbiol.* **10**, 1604
59. Garrity, J., Gardner, J. G., Hawse, W., Wolberger, C., and Escalante-Semerena, J. C. (2007) N-lysine propionylation controls the activity of propionyl-CoA synthetase. *J. Biol. Chem.* **282**, 30239–30245
60. Gardner, J. G., Grundy, F. J., Henkin, T. M., and Escalante-Semerena, J. C. (2006) Control of acetyl-coenzyme A synthetase (AcsA) activity by acetylation/deacetylation without NAD⁺ involvement in *Bacillus subtilis*. *J. Bacteriol.* **188**, 5460–5468
61. Kitata, R. B., Dimayacyac-Esleta, B. R. T., Choong, W.-K., Tsai, C.-F., Lin, T.-D., Tsou, C.-C., Weng, S.-H., Chen, Y.-J., Yang, P.-C., Arco, S. D., Nesvizhskii, A. I., Sung, T.-Y., and Chen, Y.-J. (2015) Mining missing membrane proteins by high-pH reverse-phase StageTip fractionation and multiple reaction monitoring mass spectrometry. *J. Proteome Res.* **14**, 3658–3669
62. Zhu, Y., Zou, X., Dean, A. E., Brien, J. O., Gao, Y., Tran, E. L., Park, S. H., Liu, G., Kieffer, M. B., Jiang, H., Stauffer, M. E., Hart, R., Quan, S., Satchell, K. J. F., Horikoshi, N., et al. (2019) Lysine 68 acetylation directs MnSOD as a tetrameric detoxification complex versus a monomeric tumor promoter. *Nat. Commun.* **10**, 2399
63. Zhang, X., Yuan, Z., Zhang, Y., Yong, S., Salas-Burgos, A., Koomen, J., Olashaw, N., Parsons, J. T., Yang, X. J., Dent, S. R., Yao, T. P., Lane, W. S., and Seto, E. (2007) HDAC6 modulates cell motility by altering the acetylation level of cortactin. *Mol. Cell* **27**, 197–213
64. Tang, Y., Zhao, W., Chen, Y., Zhao, Y., and Gu, W. (2008) Acetylation is indispensable for p53 activation. *Cell* **133**, 612–626
65. VanDrisse, C. M., and Escalante-Semerena, J. C. (2019) Protein acetylation in bacteria. *Annu. Rev. Microbiol.* **73**, 111–132
66. Tan, M., Peng, C., Anderson, K. A., Chhoy, P., Xie, Z., Dai, L., Park, J., Chen, Y., Huang, H., Zhang, Y., Ro, J., Wagner, G. R., Green, M. F., Madsen, A. S., Schmiesing, J., et al. (2014) Lysine glutarylation is a protein posttranslational modification regulated by SIRT5. *Cell Metab.* **19**, 605–617
67. Liu, K., Li, F., Sun, Q., Lin, N., Han, H., You, K., Tian, F., Mao, Z., Li, T., Tong, T., Geng, M., Zhao, Y., Gu, W., and Zhao, W. (2019) p53 β-hydroxybutyrylation attenuates p53 activity. *Cell Death Dis.* **10**, 243
68. Xie, Z., Zhang, D., Chung, D., Tang, Z., Huang, H., Dai, L., Qi, S., Li, J., Colak, G., Chen, Y., Xia, C., Peng, C., Ruan, H., Kirkey, M., Wang, D., et al. (2016) Metabolic regulation of gene expression by histone lysine β-hydroxybutyrylation. *Mol. Cell* **62**, 194–206
69. Sun, C. F., Xu, W. F., Zhao, Q. W., Luo, S., Chen, X. A., Li, Y. Q., and Mao, X. M. (2020) Crotonylation of key metabolic enzymes regulates carbon catabolite repression in *Streptomyces roseosporus*. *Commun. Biol.* **3**, 192
70. Sabari, B. R., Tang, Z., Huang, H., Yong-Gonzalez, V., Molina, H., Kong, H. E., Dai, L., Shimada, M., Cross, J. R., Zhao, Y., Roeder, R. G., and Allis, C. D. (2015) Intracellular crotonyl-CoA stimulates transcription through p300-catalyzed histone crotonylation. *Mol. Cell* **58**, 203–215
71. Chen, Y., Sprung, R., Tang, Y., Ball, H., Sangras, B., Kim, S. C., Falck, J. R., Peng, J., Gu, W., and Zhao, Y. (2007) Lysine propionylation and butyrylation are novel post-translational modifications in histones. *Mol. Cell. Proteomics* **6**, 812–819
72. Xu, J. Y., Xu, Z., Liu, X. X., Tan, M., and Ye, B. C. (2018) Protein acetylation and butyrylation regulate the phenotype and metabolic shifts of the endospore-forming *Clostridium acetobutylicum*. *Mol. Cell. Proteomics* **17**, 1156–1169
73. Weinert, B. T., Satpathy, S., Hansen, B. K., Lyon, D., Jensen, L. J., and Choudhary, C. (2017) Accurate quantification of site-specific acetylation stoichiometry reveals the impact of Sirtuin deacetylase CobB on the *E. coli* acetylome. *Mol. Cell. Proteomics* **16**, 759–769

74. Hansen, B. K., Gupta, R., Baldus, L., Lyon, D., Narita, T., Lammers, M., Choudhary, C., and Weinert, B. T. (2019) Analysis of human acetylation stoichiometry defines mechanistic constraints on protein regulation. *Nat. Commun.* **10**, 1055
75. Weinert, B. T., Iesmantavicius, V., Moustafa, T., Schölz, C., Wagner, S. A., Magnes, C., Zechner, R., and Choudhary, C. (2014) Acetylation dynamics and stoichiometry in *Saccharomyces cerevisiae*. *Mol. Syst. Biol.* **10**, 716
76. Sadhukhan, S., Liu, X., Ryu, D., Nelson, O. D., Stupinski, J. A., Li, Z., Chen, W., Zhang, S., Weiss, R. S., Locasale, J. W., Auwerx, J., and Lin, H. (2016) Metabolomics-assisted proteomics identifies succinylation and SIRT5 as important regulators of cardiac function. *Proc. Natl. Acad. Sci. U. S. A.* **113**, 4320–4325
77. Nishida, Y., Rardin, M. J., Carrico, C., He, W., Sahu, A. K., Gut, P., Najjar, R., Fitch, M., Hellerstein, M., Gibson, B. W., and Verdin, E. (2015) SIRT5 regulates both cytosolic and mitochondrial protein malonylation with glycolysis as a major target. *Mol. Cell* **59**, 321–332
78. Schilling, B., Christensen, D., Davis, R., Sahu, A. K., Hu, L. I., Walker-Peddakotla, A., Sorensen, D. J., Zemaitaitis, B., Gibson, B. W., and Wolfe, A. J. (2015) Protein acetylation dynamics in response to carbon overflow in *Escherichia coli*. *Mol. Microbiol.* **98**, 847–863
79. Basisty, N., Meyer, J. G., Wei, L., Gibson, B. W., and Schilling, B. (2018) Simultaneous quantification of the acetylome and succinylome by 'one-pot' affinity enrichment. *Proteomics* **18**, 1800123
80. Cao, J., Wang, T., Wang, Q., Zheng, X., and Huang, L. (2019) Functional insights into protein acetylation in the hyperthermophilic archaeon *Sulfolobus islandicus*. *Mol. Cell. Proteomics* **18**, 1572–1587
81. Zhang, D., Tang, Z., Huang, H., Zhou, G., Cui, C., Weng, Y., Liu, W., Kim, S., Lee, S., Perez-Neut, M., Ding, J., Czyz, D., Hu, R., Ye, Z., He, M., et al. (2019) Metabolic regulation of gene expression by histone lactylation. *Nature* **574**, 575–580
82. Rajasekaran, N. S., Connell, P., Christians, E. S., Yan, L. J., Taylor, R. P., Orosz, A., Zhang, X. Q., Stevenson, T. J., Peshock, R. M., Leopold, J. A., Barry, W. H., Loscalzo, J., Odelberg, S. J., and Benjamin, I. J. (2007) Human α B-crystallin mutation causes oxido-reductive stress and protein aggregation cardiomyopathy in mice. *Cell* **130**, 427–439
83. Trotter, E. W., and Grant, C. M. (2002) Thioredoxins are required for protection against a reductive stress in the yeast *Saccharomyces cerevisiae*. *Mol. Microbiol.* **46**, 869–878
84. Sauve, A. A., Wolberger, C., Schramm, V. L., and Boeke, J. D. (2006) The biochemistry of sirtuins. *Annu. Rev. Biochem.* **75**, 435–465
85. Anderson, K. A., Huynh, F. K., Fisher-Wellman, K., Stuart, J. D., Peterson, B. S., Douros, J. D., Wagner, G. R., Thompson, J. W., Madsen, A. S., Green, M. F., Sivley, R. M., Ilkayeva, O. R., Stevens, R. D., Backos, D. S., Capra, J. A., et al. (2017) SIRT4 is a lysine deacetylase that controls leucine metabolism and insulin secretion. *Cell Metab.* **25**, 838–855.e15
86. Pannek, M., Simic, Z., Fuszard, M., Meleshin, M., Rotili, D., Mai, A., Schutkowski, M., and Steegborn, C. (2017) Crystal structures of the mitochondrial deacetylase Sirtuin 4 reveal isoform-specific acyl recognition and regulation features. *Nat. Commun.* **8**, 1513
87. Colak, G., Xie, Z., Zhu, A. Y., Dai, L., Lu, Z., Zhang, Y., Wan, X., Chen, Y., Cha, Y. H., Lin, H., Zhao, Y., and Tan, M. (2013) Identification of lysine succinylation substrates and the succinylation regulatory enzyme CobB in *Escherichia coli*. *Mol. Cell. Proteomics* **12**, 3509–3520
88. Ringel, A. E., Roman, C., and Wolberger, C. (2014) Alternate deacetylating specificities of the archaeal sirtuins Sir2A1 and Sir2A2. *Protein Sci.* **23**, 1686–1697
89. Gallus, C., and Schink, B. (1994) Anaerobic degradation of pimelate by newly isolated denitrifying bacteria. *Microbiology* **140**, 409–416
90. Harrison, F. H., and Harwood, C. S. (2005) The pimFABCDE operon from *Rhodospseudomonas palustris* mediates dicarboxylic acid degradation and participates in anaerobic benzoate degradation. *Microbiology* **151**, 727–736
91. Schöcke, L., and Schink, B. (1999) Energetics and biochemistry of fermentative benzoate degradation by *Syntrophus gentianae*. *Arch. Microbiol.* **171**, 331–337
92. Müller, N., Worm, P., Schink, B., Stams, A. J. M., and Plugge, C. M. (2010) Syntrophic butyrate and propionate oxidation processes: From genomes to reaction mechanisms. *Environ. Microbiol. Rep.* **2**, 489–499
93. Boll, M., Geiger, R., Junghare, M., and Schink, B. (2020) Microbial degradation of phthalates: Biochemistry and environmental implications. *Environ. Microbiol. Rep.* **12**, 3–15